Turbulent length scales and Reynolds stress anisotropy in wall-wake flow downstream of an isolated dunal bedform

Subhasish Dey and Sankar Sarkar

Subhasish Dey

Department of Civil Engineering
Indian Institute of Technology Kharagpur
India

1

Introduction

Natural turbulent streams often come across bed-mounted solid obstacles of different geometries that play an important role in modifying flow characteristics

These obstacles are often called *bluff-bodies*

A bed-mounted bluff-body in a streamflow generates wake at its downstream called *wall-wake flow*

The wake flow downstream of a bluff-body remains a topic of immense importance in applied hydrodynamics. However, inadequate attention has so far been paid to study isolated dunal bedform as a bluff-body and the turbulence characteristics (particularly, turbulent length scales and Reynolds stress anisotropy) in wall-wake

Objective of the Present Study

To characterize the turbulent flow downstream of an isolated dunal bedform mounted on a rough bed

Attention has been paid principally on

- the streamwise velocity, Reynolds shear stress and average turbulence intensity

- the turbulent length scales (Prandtl's mixing length, Taylor microscale and Kolmogorov length scale)

- the Reynolds stress anisotropy

Experimental Setup

Fig. 1 Photographs of the dunal structures for (a) Run 1 and (b) Run 2
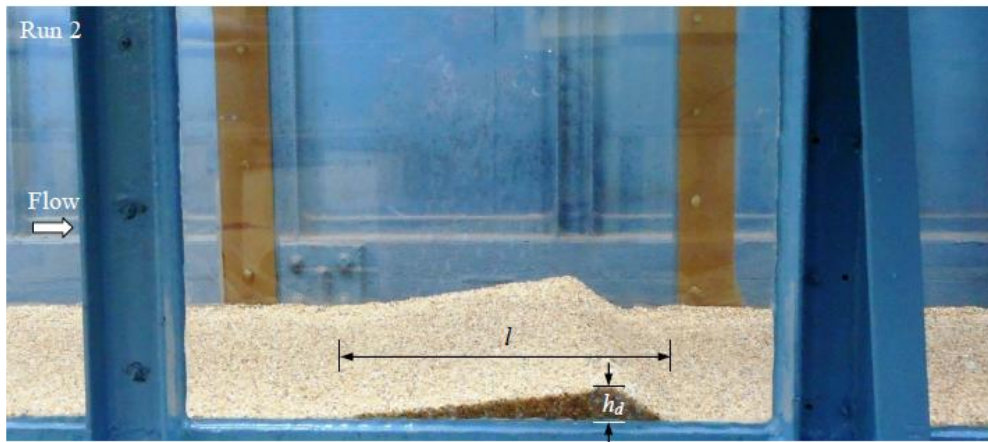
Experiments were performed in a rectangular flume of 20 m long, 0.5 m wide and 0.5 m high for two dunal structures

Run 1:
$h_d = 0.09$ m
$l = l_s + l_L = 0.24 + 0.16 = 0.4$ m

Run 2:
$h_d = 0.03$ m
$l = l_s + l_L = 0.24 + 0.06 = 0.3$ m

4

Experimental Parameters

Run	h (m)	d_{50} (mm)	$\overline{U}$ (m s^{-1})	S (%)	$u_{*1,S}$ (m s^{-1})	$u_{*2,RSS}$ (m s^{-1})	R	F	R_*
1	0.30	2.49	0.44	0.03	0.030	0.027	5.28×10^5	0.256	74.7
2	0.30	2.49	0.44	0.03	0.030	0.025	5.28×10^5	0.256	74.7

h = flow depth

d_{50} = median size of gravel

u_* = approach shear velocity

R_* = shear-particle Reynolds number ($= d_{50}u_*/\nu$)

ν = coefficient of kinematic viscosity of water

$\overline{U}$ = depth-averaged approach velocity

S = bed slope

R = Reynolds number ($= 4\overline{U}h/\nu$)

F = Froude number ($= \overline{U}/(gh)^{0.5}$)

Measurements

Fig. 2 Vectrino

Sampling rate: 100 Hz

Sampling volume: 6 mm diameter

Height: 1–4 mm

Duration of sampling: 300 s
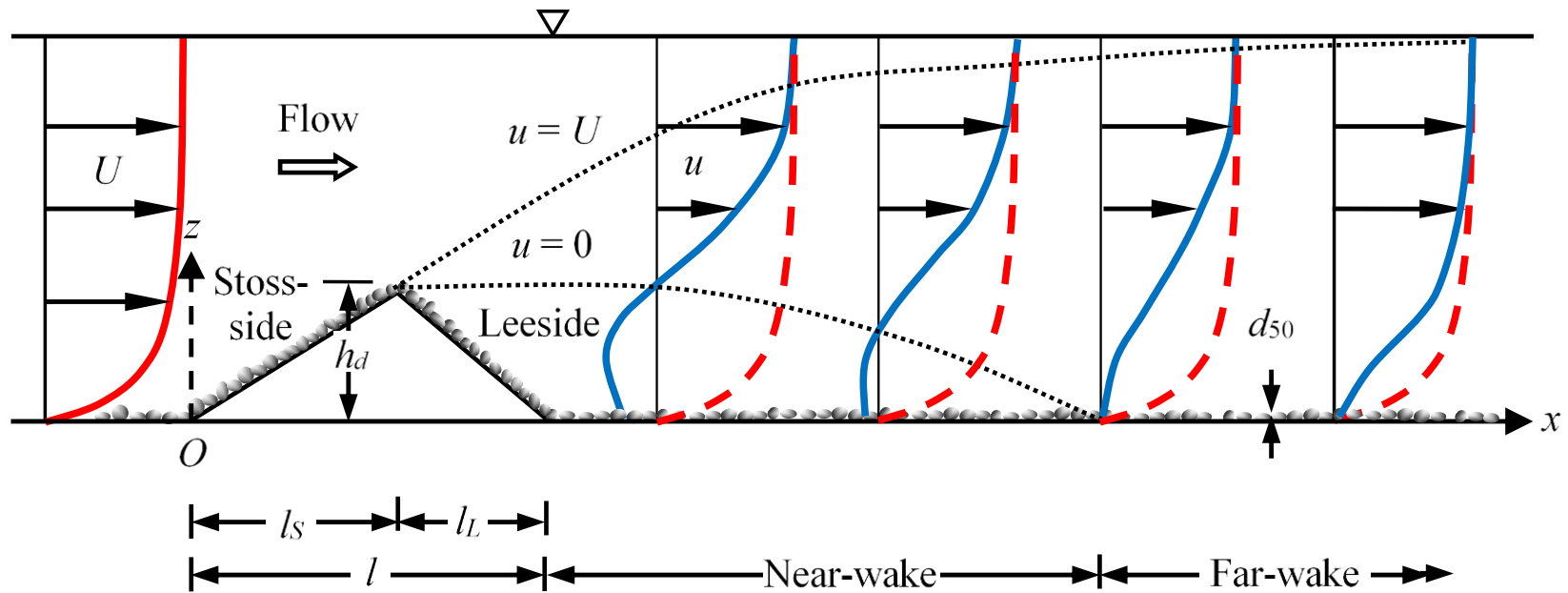
Vectrino signal correlation values: $\geq 70\%$

SNR (signal-to-noise ratio): ≥ 17

Spike removal: *Acceleration thresholding method*

Locations of velocity measurements: $x/l = -0.5$, -0.25, 0, 0.1, 0.2, 0.3, 0.4, 0.5, 0.6, 0.7, 0.8, 0.9, 1, 1.1, 1.3, 1.7, 2.1, 2.5 and 3.3; where $l = l_s + l_l$

u, v and w: Velocity components in the streamwise (x), spanwise (y) and vertical (z) directions, respectively

Fig. 3 Schematic of an isolated dunal bedform and velocity profiles

Definition Sketch

Immediate downstream vicinity of the dune, the flow is characterized by the reversed flow (up to the reattachment point), called the *near-wake flow*

Thereafter, the flow is called the *far-wake flow*

The upper dotted line represents the boundary layer ($u = U$) in wall-wake flow and the lower dotted line signifies the locus of null velocity ($u = 0$), where $u(z)$ is the streamwise velocity in wake flow and $U(z)$ is the streamwise velocity in undisturbed upstream flow

The far-wake flow having a defect in velocity profiles stars recovering, as the flow travels downstream

Far downstream, the flow fully recovers the undisturbed upstream flow
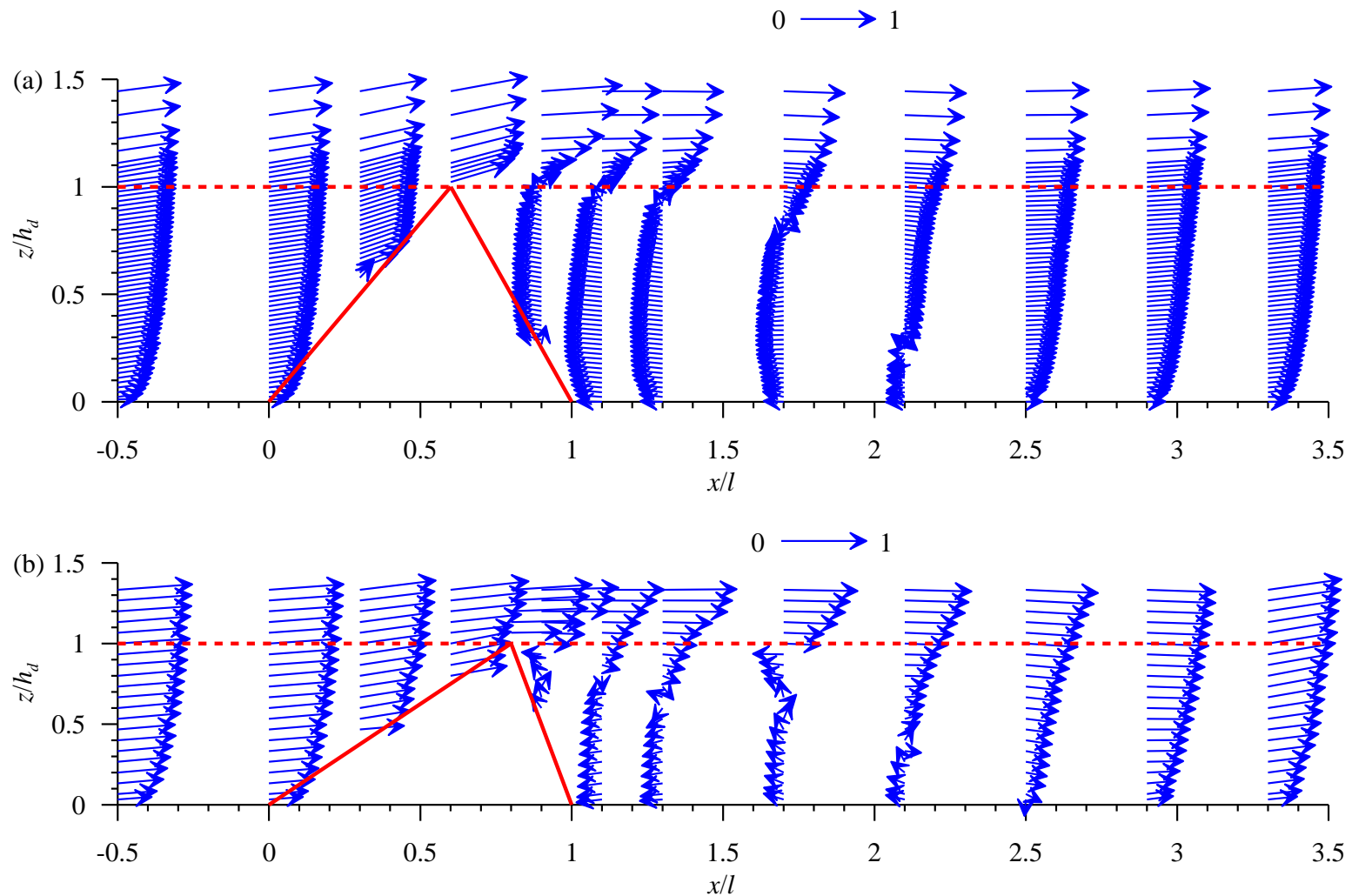
Fig. 4 Velocity vectors in flows upstream and downstream of an isolated dune for (a) Run 1 and (b) Run 2

9

Upstream of the dune, the velocity vectors do not change significantly in magnitude and direction while approaching

Immediate downstream vicinity of the dune ($1 \leq x/l \leq 1.75$), the velocity vectors change their directions, signifying a circulatory motion in the near-wake flow zone

The wall-wake flow starts recovering the undisturbed upstream flow with an increase in horizontal distance, attaining the undisturbed velocity vectors at far downstream ($x/l = 3.3$)
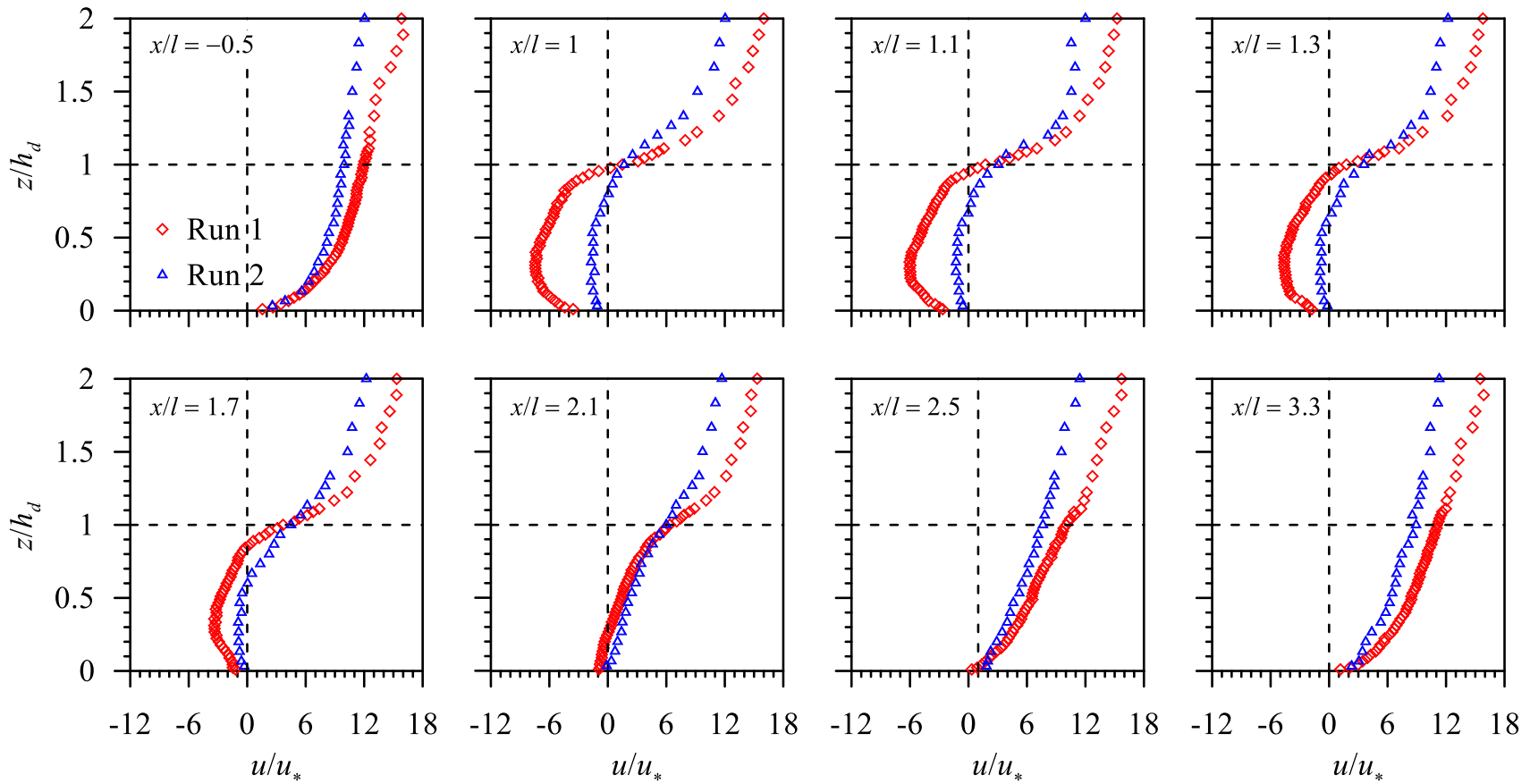
Fig. 5 Vertical profiles of nondimensional streamwise velocity u/u_* at different streamwise distances for Runs 1 and 2

The approach shear flow passing the isolated dune gets separated to form a reversed flow, in the near-wake flow zone, at the immediate downstream vicinity of the dune ($1 \leq x/l \leq 1.5$)

At downstream, the reversed flow disappears establishing the far-wake flow ($1.5 < x/l < 3.3$)

Far downstream of the dune ($x/l \geq 3.3$), the velocity profiles recover their respective undisturbed upstream profiles

Here, τ is the Reynolds shear stress relative to mass density ρ of water, defined by $-\overline{u'w'}$
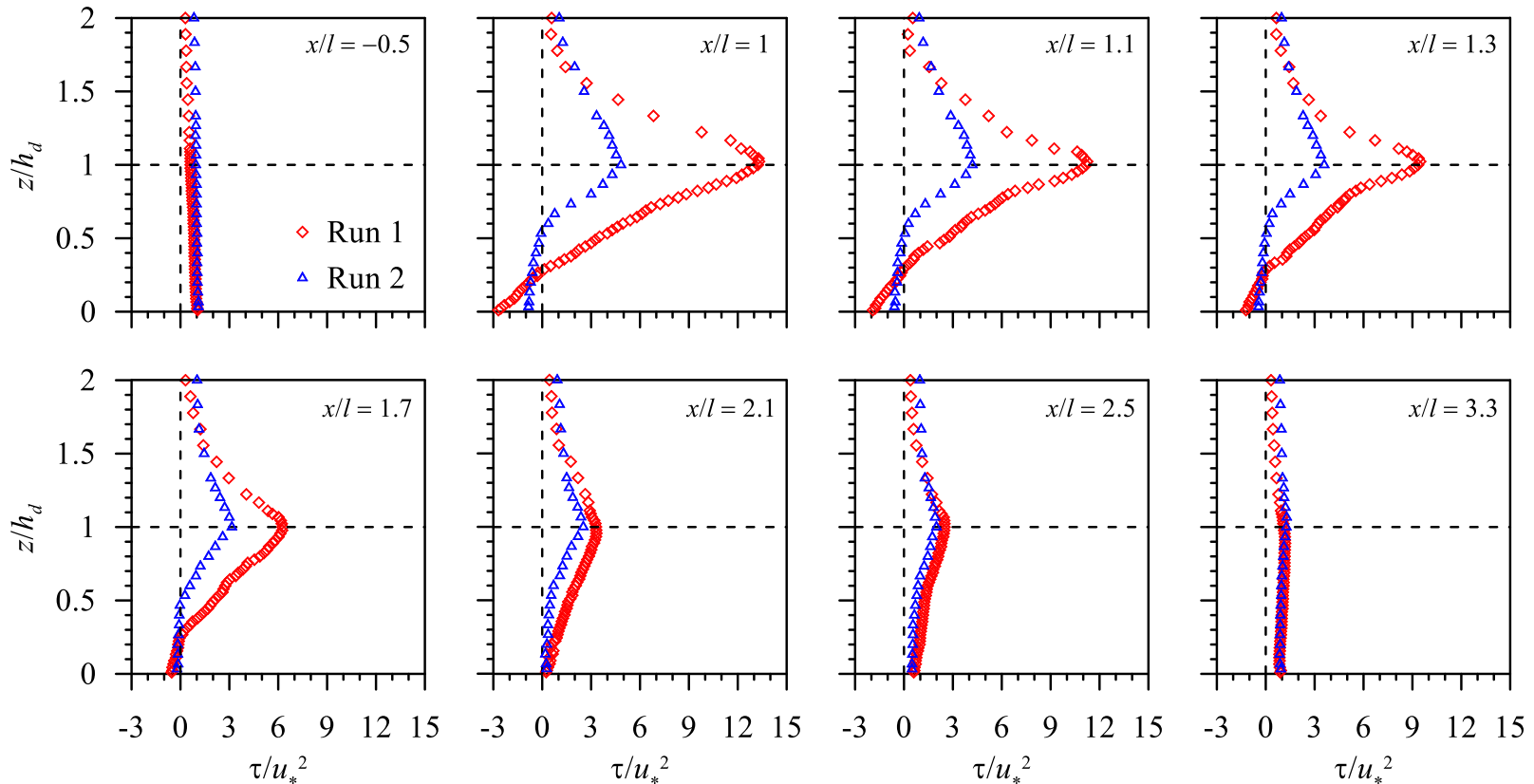
Fig. 6 Vertical profiles of nondimensional RSS at different streamwise distances for Run 1 and Run 2
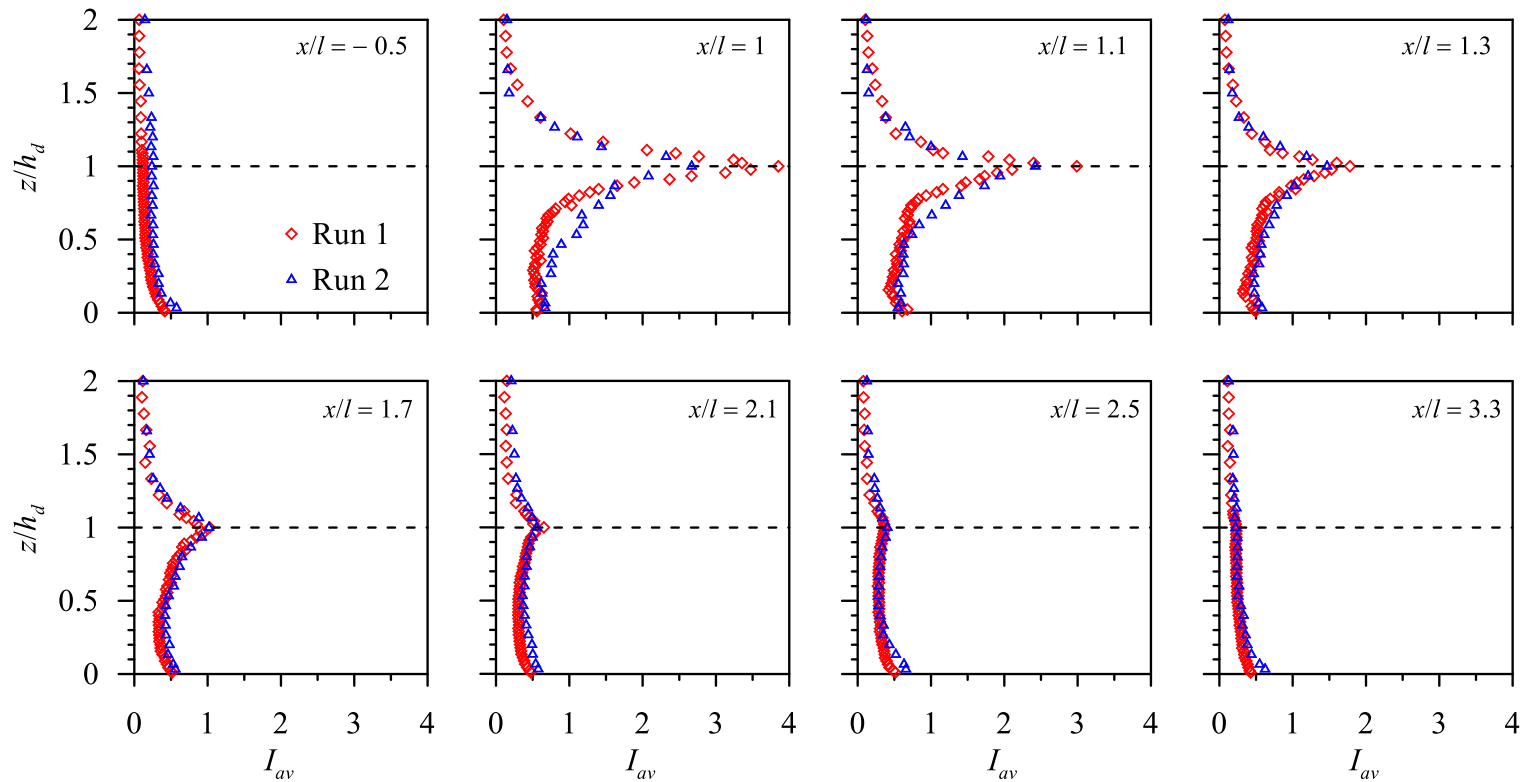
Upstream of the dune ($x/l = -0.5$), the RSS profiles follow a linear law

Downstream of the dune, the RSS profiles start with a finite value from the bed and increase with an increase in vertical distance until they attain their peaks at the dune crest. Then, they decrease, as one goes toward the free surface

The peaks in RSS profiles progressively diminish with an increase in downstream distance

Far downstream of the dune ($x/l = 3.3$), the RSS profiles follow the undisturbed upstream profiles, confirming a stress recovery

Here, $I_{av} = (2q/3)^{0.5}/U_1$; where q is the turbulent kinetic energy (TKE), U_1 is the local time-averaged resultant velocity [$= (u^2 + v^2 + w^2)^{0.5}$]

Fig. 7 Vertical profiles of average turbulence intensity I_{av} at different streamwise distances for Runs 1 and 2

15

Upstream of the dune ($x/l = -0.5$), the I_{av} profiles start with high-turbulence level (0.05−0.2) induced from the near bed. As the vertical distance increases, the I_{av} profiles gradually reduces to medium (0.01−0.05) and then to low (less than 0.01) turbulence ranges

Downstream of the dune, the I_{av} profiles start with a high-turbulence level close to the bed

After a brief decrease, the I_{av} profiles increase sharply with vertical distance, attaining their peak values at the dune crest

Turbulent Length Scales

Fig. 8 Energy cascade process

Big whorls have little whorls;
which feed on their velocity;
and little whorls have lesser whorls;
and so on to viscosity
(in the molecular sense)
[Richardson 1922]

17

Prandtl's Mixing-Length

The eddies forming the fluid parcels generate and then degenerate to exchange their momentum after travelling an average distance, termed the *mixing length* (also well-known as *Prandtl's mixing length*)
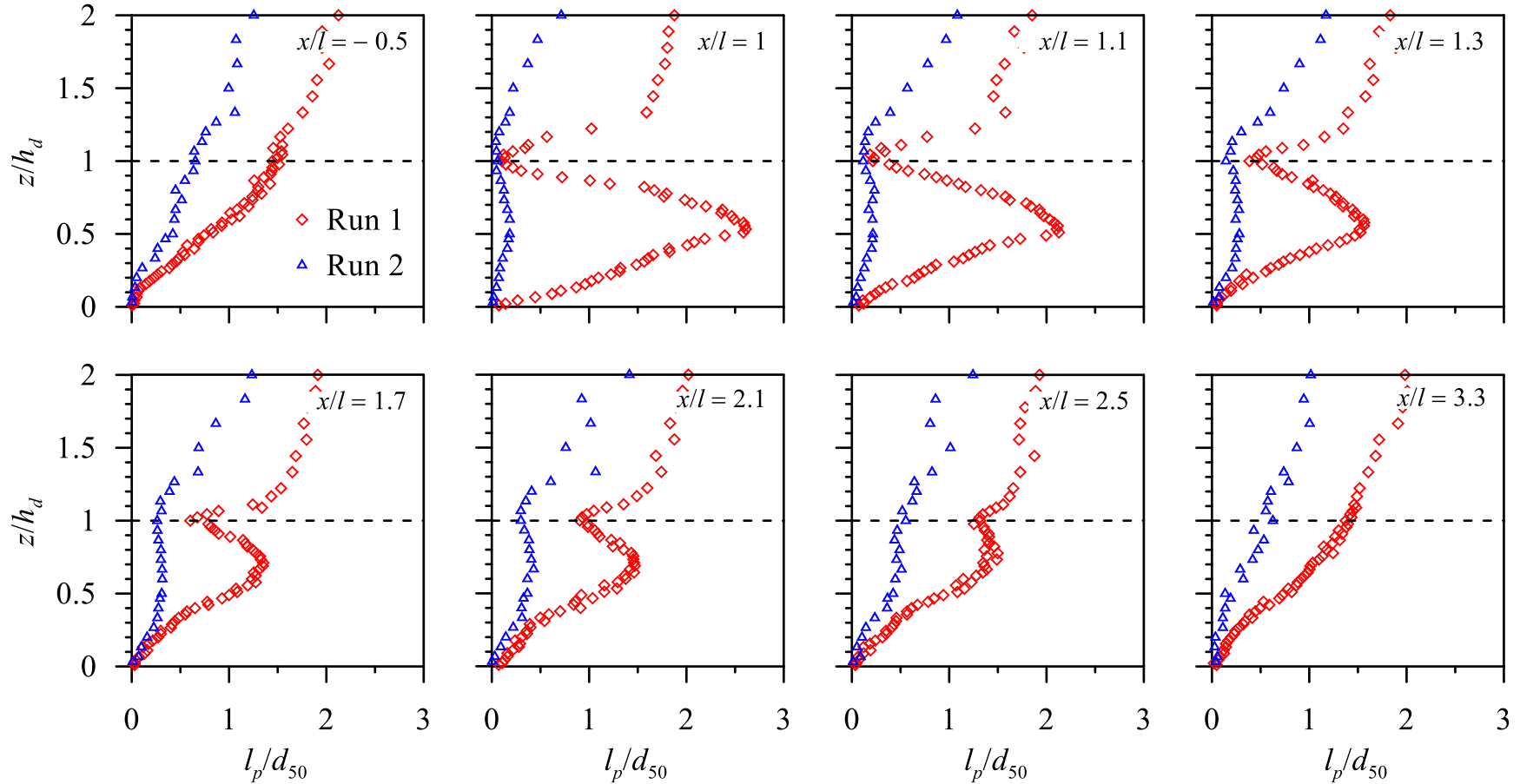
The Prandtl's mixing length *l* is calculated as

$$l_p(z) = \frac{(-\overline{u'w'})^{0.5}}{d\overline{u}/dz}$$

1

u' and w' = fluctuations of u and w with respect to their time averaged values

The overbar denotes the time-averaged quantity

Fig. 9 Vertical profiles of nondimensional Prandtl's mixing length l_p/d_{50} at different streamwise distances for Runs 1 and 2

Upstream of the dune ($x/l = -0.5$), the l_p/d_{50} profiles increase almost linearly with an increase in vertical distance obeying $l_p = \kappa z$

Downstream of the dune ($x/l \geq 1$), the l_p/d_{50} profiles increase sharply with an increase in vertical distance, attaining their peak values at $z/h_d \approx 0.5$–0.6

Then, they decrease to a second lowest critical value at the dune crest ($z/h_d \approx 1$) and thereafter, gradually increase, as one goes toward the free surface

Far downstream of the dune ($x/l = 3.3$), the l_p/d_{50} profiles become almost similar to their undisturbed upstream profiles displaying a recovery of mixing-length
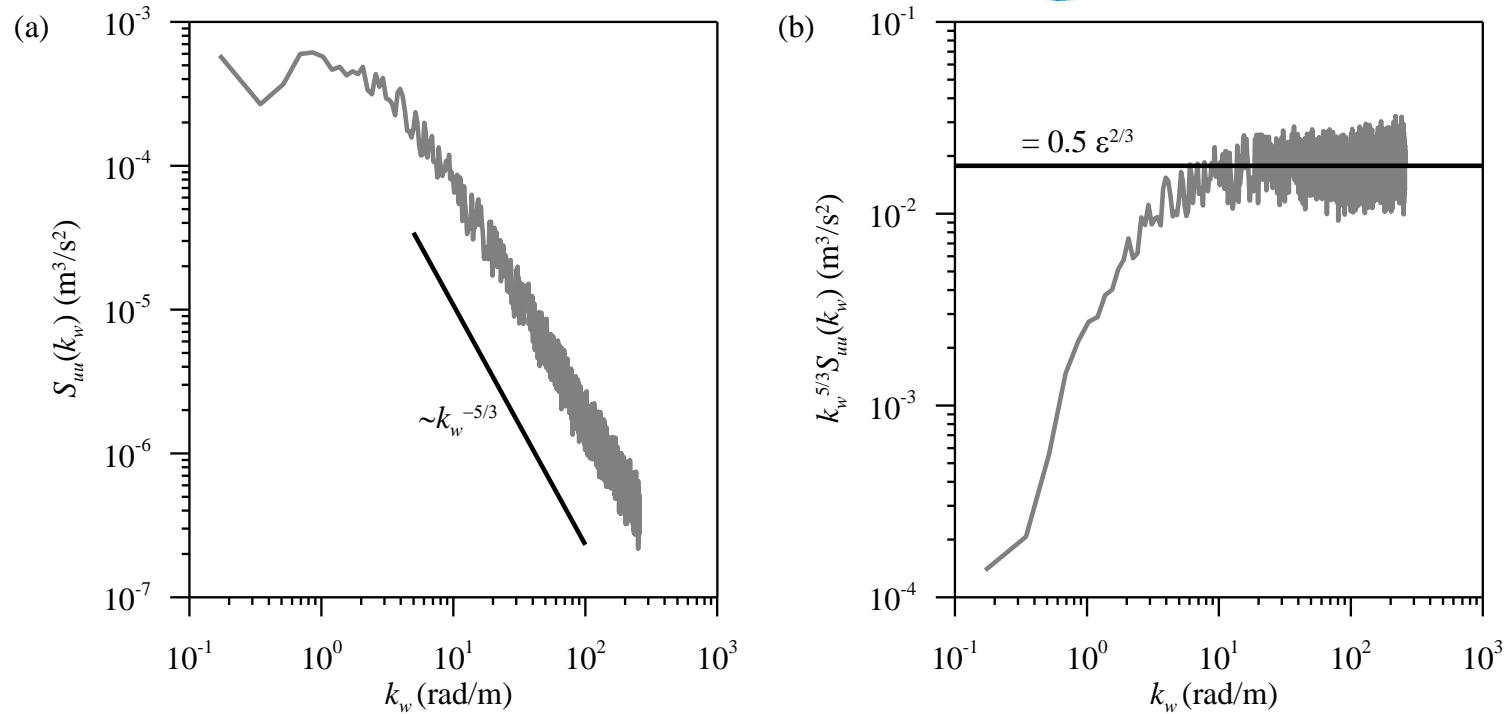
Taylor Microscale

Taylor microscale λ defines a typical eddy size in the inertial subrange

It is given by

$$\lambda = \left(\frac{15 \upsilon \sigma_u}{\varepsilon} \right)^{0.5}$$

2

where σ_u is the streamwise Reynolds normal stress divided by ρ that is $\overline{u'u'}$ and ε is the TKE dissipation rate. The ε was estimated from the Kolmogorov second hypothesis

Fig. 10. (a) Velocity power spectrum $S_{uu}(k_w)$ and (b) determination of ε

Velocity spectra display portions of constant $k_w^{-5/3}$ slope at higher frequencies suggesting the inertial subrange. TKE dissipation rate ε is calculated from Fig. 10(b)
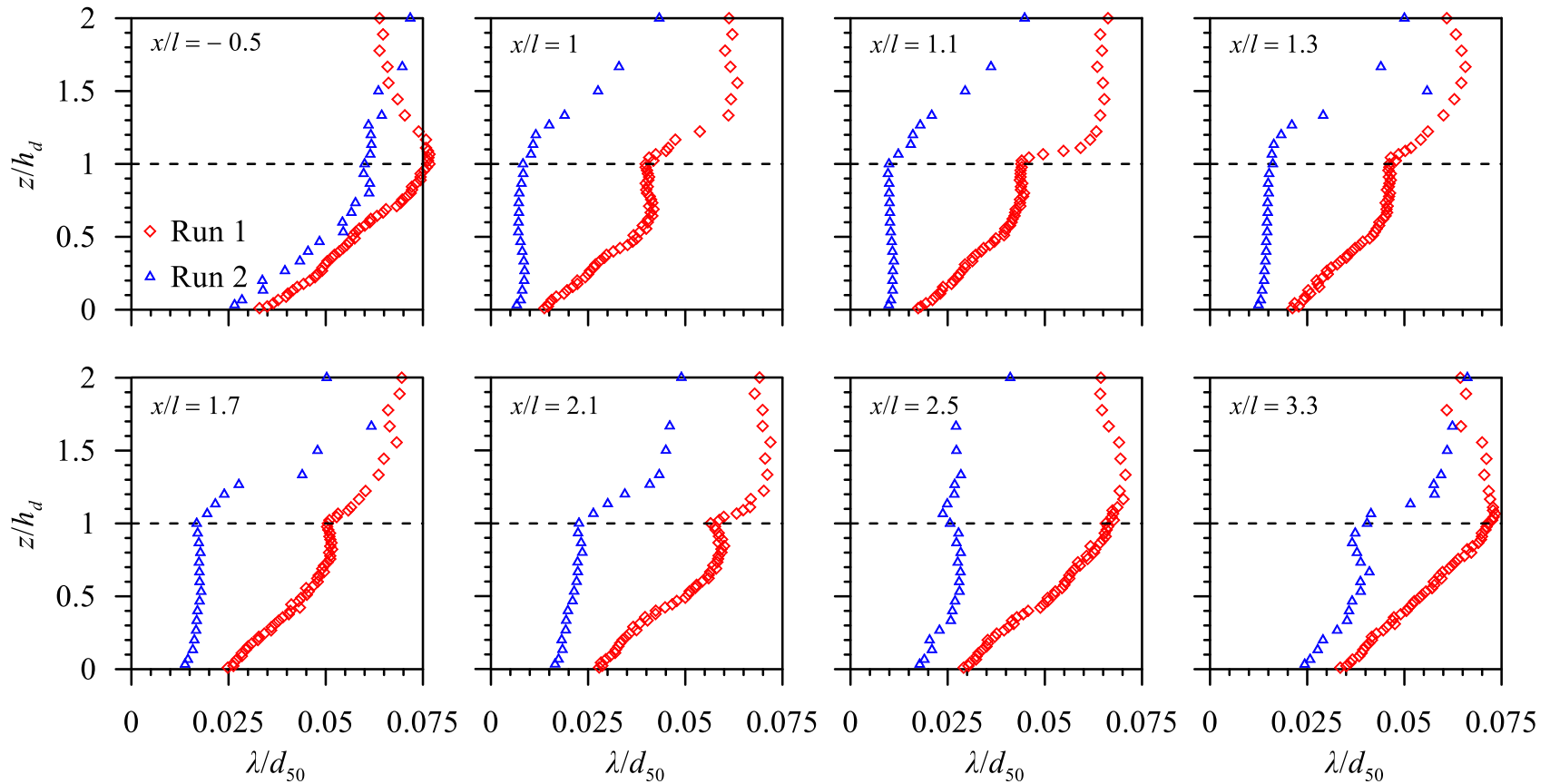
Fig. 11 Vertical profiles of nondimensional Taylor microscale λ/d_{50} at different streamwise distances for Runs 1 and 2

Upstream of the dune, the λ/d_{50} profiles gradually increase with an increase in vertical distance up to $z/h_d \approx 1.25$ and thereafter become almost invariant with the vertical distance, as one goes toward free surface

Downstream of the dune, the λ/d_{50} profiles increase gradually with vertical distance up to $z/h_d \approx 0.75$ and then, decrease sharply up to the dune crest

Above the crest, they again start increasing and becoming almost invariant to vertical distance as one goes toward the free surface
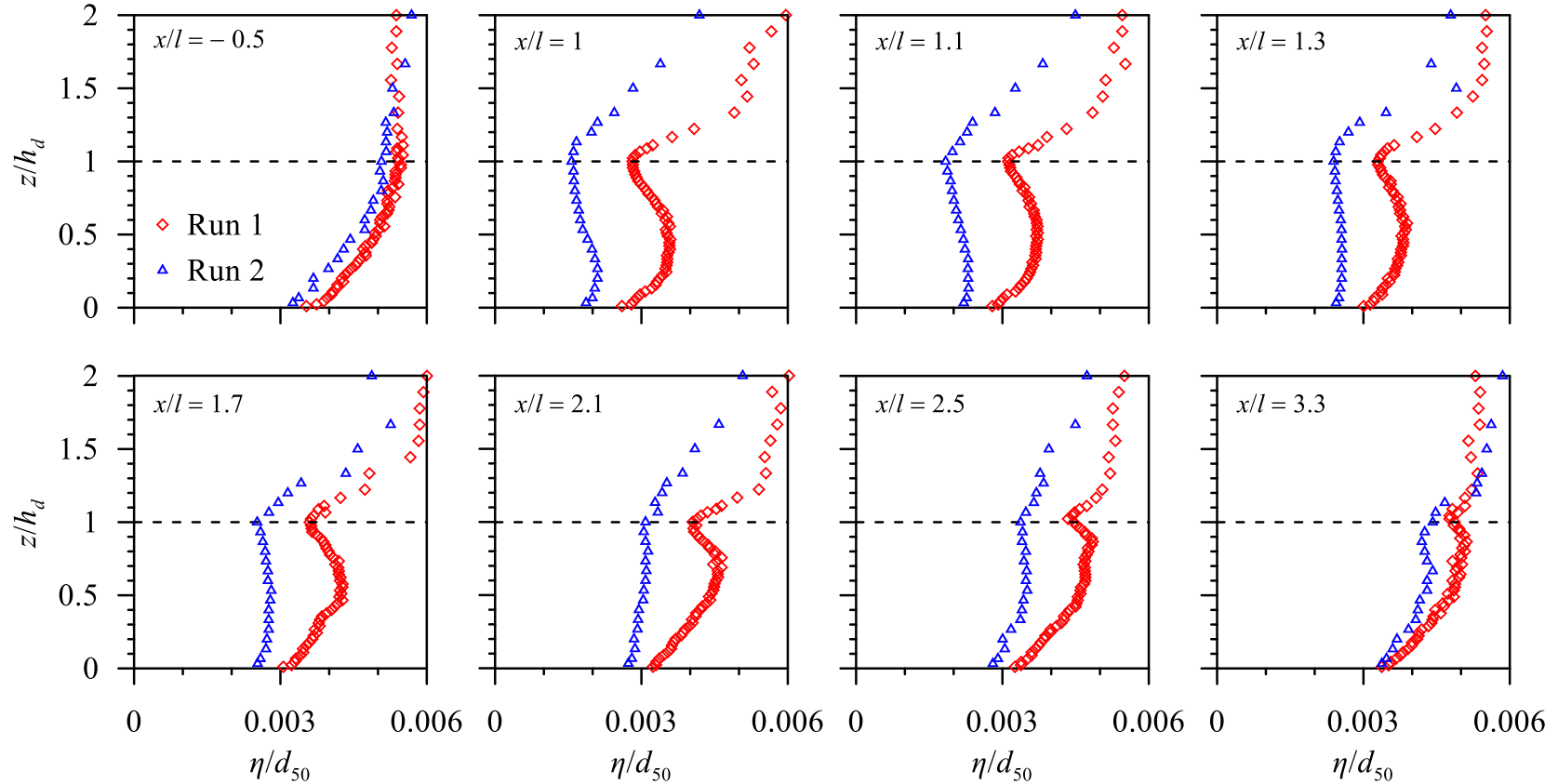
Kolmogorov Length Scale

In the dissipation range, the viscosity dominates and the TKE is dissipated into heat. The dissipation of TKE takes place at a length scale of the order of Kolmogorov length scale η

It is given by

$$\eta = (\upsilon^3 / \varepsilon)^{0.25}$$

3

Fig. 12 Vertical profiles of nondimensional Kolmogorov length scale η/d_{50} at different streamwise distances for Runs 1 and 2

The characteristics of the distributions of Kolmogorov length scale are almost similar to those of Taylor microscale, having a different magnitude

At a given vertical distance, the Kolmogorov length scale in wall-wake flow is approximately 1/10 times the Taylor microscale

Anisotropy Analysis

In an *isotropic turbulence*, the velocity fluctuations in a turbulent fluid flow are independent of the axis of reference and invariant to the rotation of axis
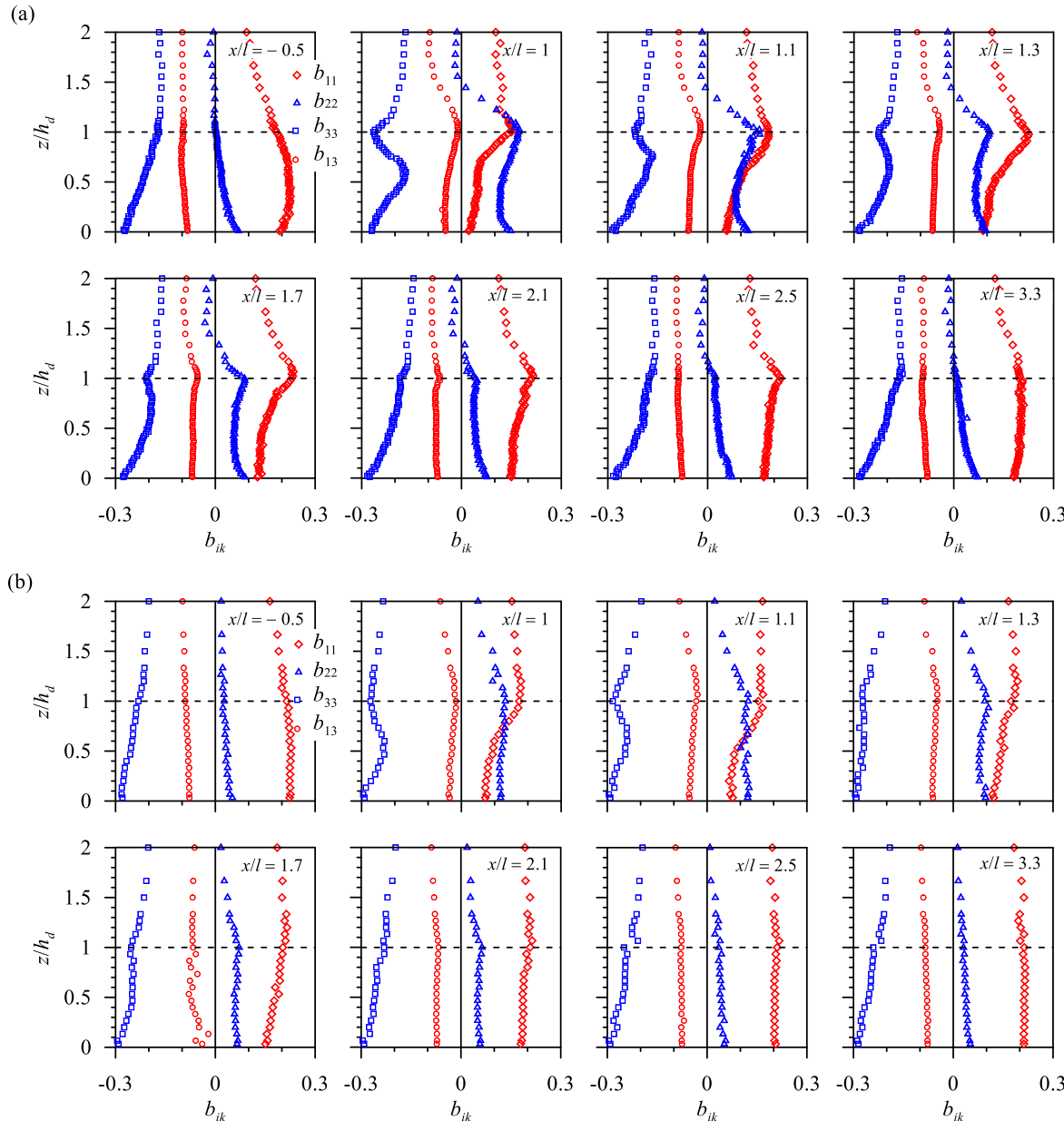
Reynolds stress anisotropy tensor b_{ik} is defined as the difference between the ratio of Reynolds stress tensor terms to the turbulent kinetic energy and its isotropic equivalence

$$b_{ik} = \overline{u'_i u'}_k / (2q) - \delta_{ik} / 3 \qquad \textbf{4}$$

where q is the average turbulent kinetic energy and δ_{ik} is the Kronecker delta function $\delta_{ik} = 0$ if $i \neq k$, or 1 if $i = k$

The b_{ik} remains a symmetric and traceless tensor ranging from $-1/3$ to $2/3$ and vanishes for an isotropic turbulence ($b_{ik} = 0$)

Fig. 13 Vertical profiles of Reynolds stress anisotropy tensor b_{ik} at different streamwise distances for (a) Run 1 and (b) Run 2

29

Downstream of the dune, the b_{11} and b_{22} components suggest the wall-wake flow yields less anisotropic turbulence in streamwise direction and more in spanwise direction below the crest

On the other hand, the b_{33} component produces more anisotropic turbulence in the lower half and less in the upper half of the dune, as compared to their undisturbed upstream values. However, the b_{13} component, signifies the ratio of RSS to TKE, exhibits little change in wall-wake flow

For all b_{ik} components, they display a kink at the crest level. However, a recovery is evident, as downstream distance increases
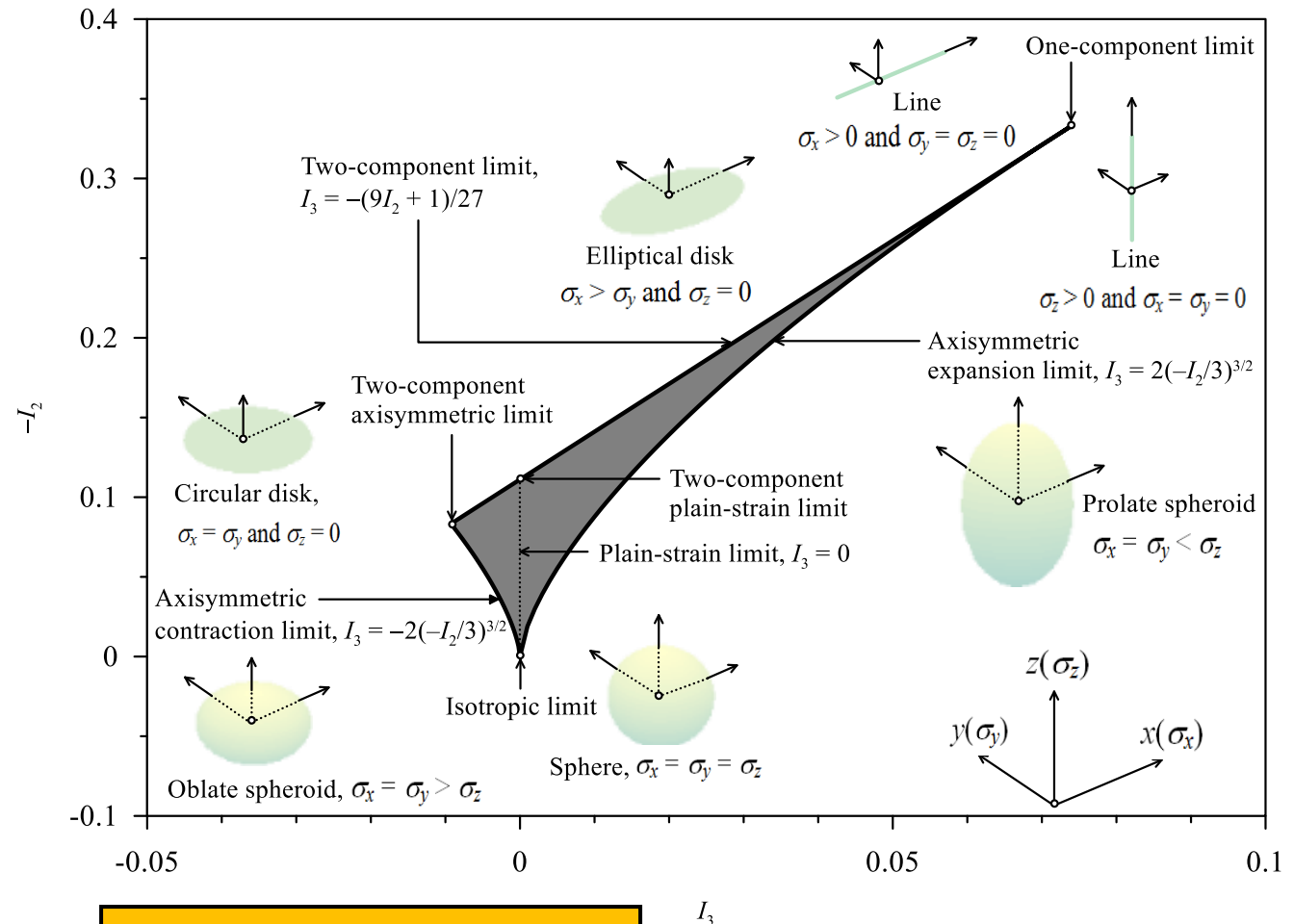
Lumley Triangle

A convenient method for comparing the overall anisotropy is to use two principal invariants:

$$I_2 = \left(b_{ik} b_{ik} / 2 \right)$$
$$I_3 = b_{ij} b_{jk} b_{ki} / 3$$

John Lumley
(1930–2015)

Fig. 14 Lumley triangle

31

A quantitative description of total Reynolds stress anisotropy is ascertained by plotting $-I_2$ against I_3, termed *anisotropy invariant map* (AIM). In an AIM, $-I_2$ (positive or zero) represents the degree of anisotropy and I_3 refers to the nature of anisotropy
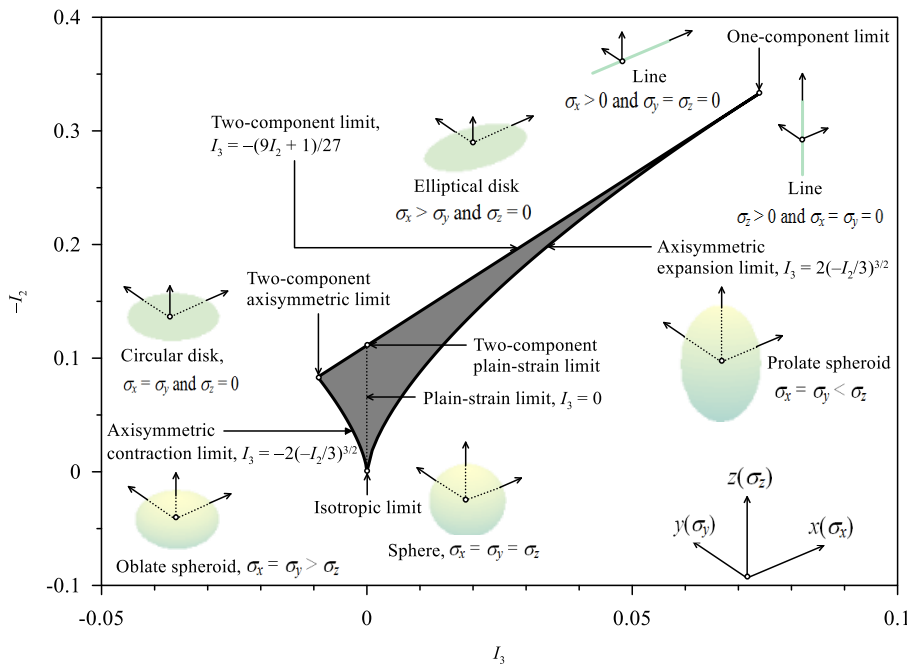
The left-curved and the right-curved boundaries, being symmetric about the *plane-strain limit* ($I_3 = 0$), evolve from the isotropic limit ($I_2 = I_3 = 0$), obeying a generic relationship as $I_3 = \pm 2(-I_2/3)^{3/2}$
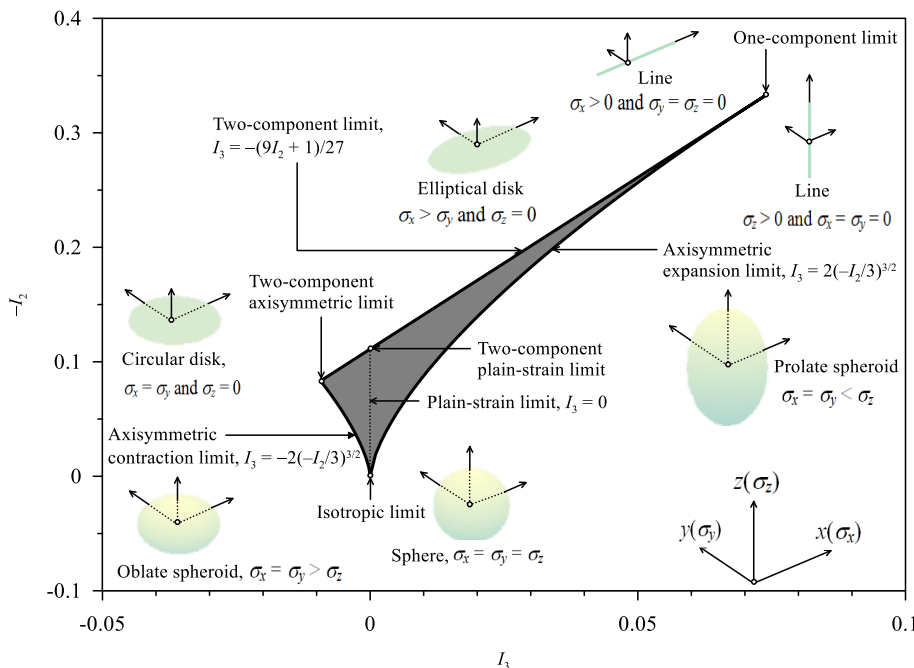
The top-linear boundary follows the relationship $I_3 = -(9I_2 + 1)/27$

For an isotropic turbulence ($I_2 = I_3 = 0$ or $\sigma_x = \sigma_y = \sigma_z$), the stress ellipsoid is a sphere

The left-curved boundary corresponds to the *axisymmetric contraction limit*, where one component of Reynolds normal stress is smaller than the other two components that are equal ($\sigma_x = \sigma_y > \sigma_z$). The stress ellipsoid becomes an oblate spheroid. At the left vertex, corresponding to the *two-component axisymmetric limit*, one component of Reynolds normal stress vanishes leaving the other two equal components ($\sigma_x = \sigma_y$ and $\sigma_z = 0$). The stress ellipsoid is a circular disc


The right-curved boundary corresponds to the *axisymmetric expansion limit*, where one component of Reynolds normal stress is larger than the remaining two components that are equal ($\sigma_x = \sigma_y < \sigma_z$). The stress ellipsoid is a prolate spheroid

33

The top-linear boundary corresponds to the *two-component limit*, because one component of Reynolds normal stress is larger than the other component in conjunction with a third component that disappears ($\sigma_x > \sigma_y$ and $\sigma_z = 0$). This makes the stress ellipsoid an elliptical disk

The intersecting point of the two-component limit and the plain-strain limit is called *two-component plain-strain limit*
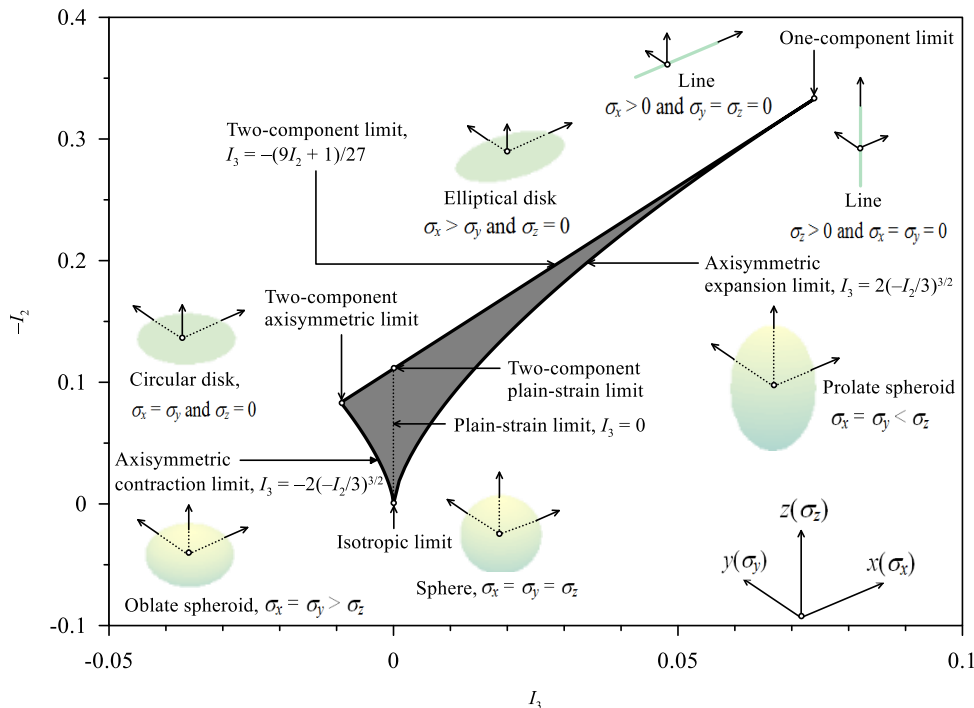
At the right vertex, corresponding to the *one-component limit* [($\sigma_x > 0$, $\sigma_y = \sigma_z = 0$) or ($\sigma_x = \sigma_y = 0$, $\sigma_z > 0$)], one component of Reynolds normal stress prevails along with the other two vanishing components. It results a stress ellipsoid to become a line
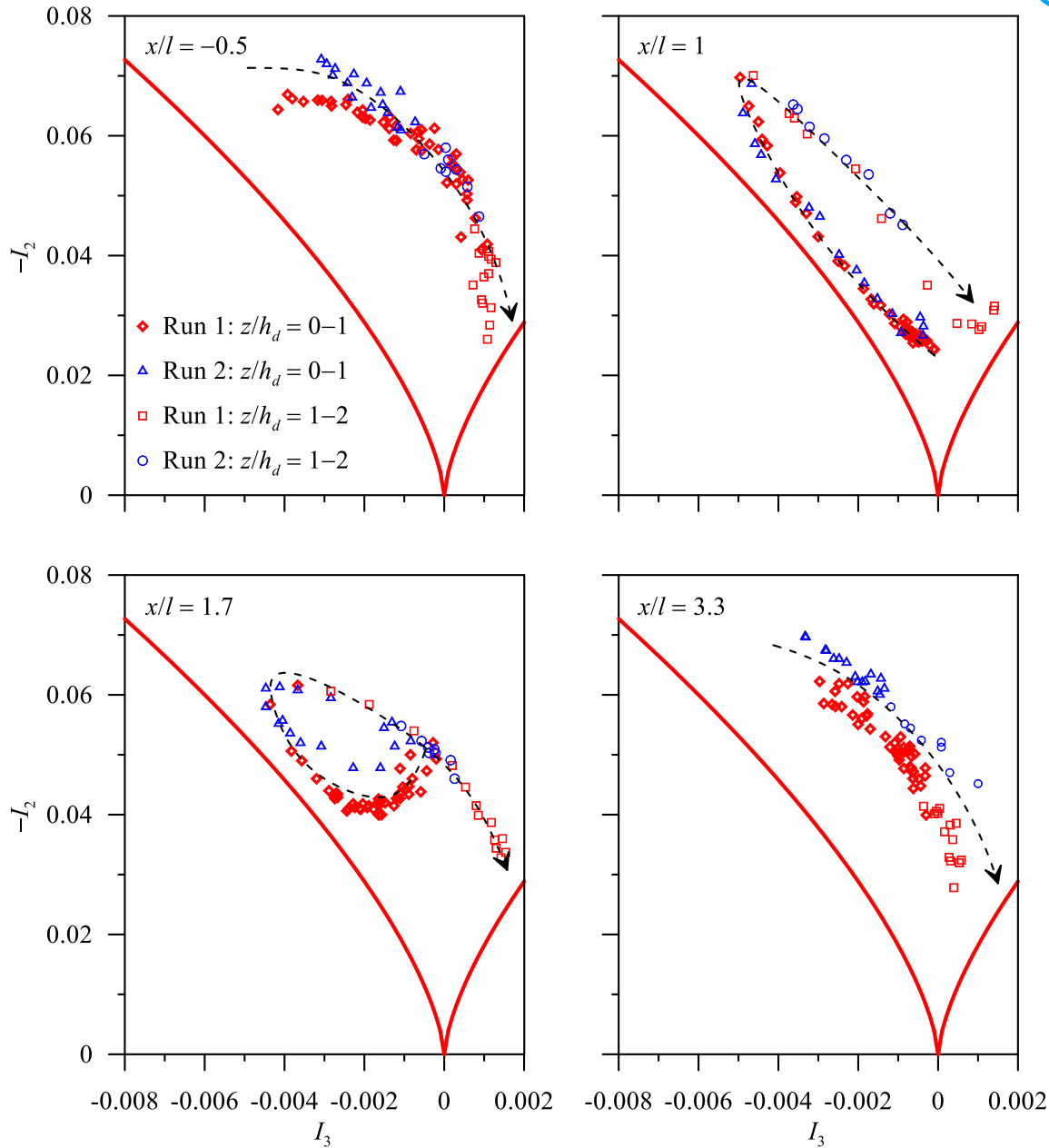
Fig. 15 AIMs at different streamwise distances for Runs 1 and 2

Upstream of the dune ($x/l = -0.5$), the data plots show that the anisotropy has a tendency to reduce toward a quasi-three-dimensional isotropy, as the vertical distance increases

Immediate downstream of the dune, the data plots have a tendency to form a stretched loop inclined to the left-curved boundary. Below the crest ($z/h_d < 1$), the turbulence anisotropy is to have an affinity toward a two-dimensional isotropy

The reason is attributed to the fact that the vertical velocity fluctuations are less than both the streamwise and the spanwise velocity fluctuations that are approximately equal

Above the crest, the turbulence anisotropy tend to reduce toward a quasi-three-dimensional isotropy

Further downstream ($x/l = 1.7$), the loop formed by the data plots reduces its size forming a tail and finally disappears at far downstream ($x/l = 3.3$), corroborating a recovery of the undisturbed upstream trend

In the wall-wake flow, below the crest, the turbulence is characterized with an affinity to show a two-dimensional isotropy, while above the crest, the anisotropy has a tendency to reduce to a quasi-three-dimensional isotropy

The axisymmetric contraction to the oblate spheroid increases with an increase in vertical distance up to the crest. Above the crest, the axisymmetric contraction to oblate spheroid relaxes with a further increase in vertical distance

Anisotropy Invariant Function
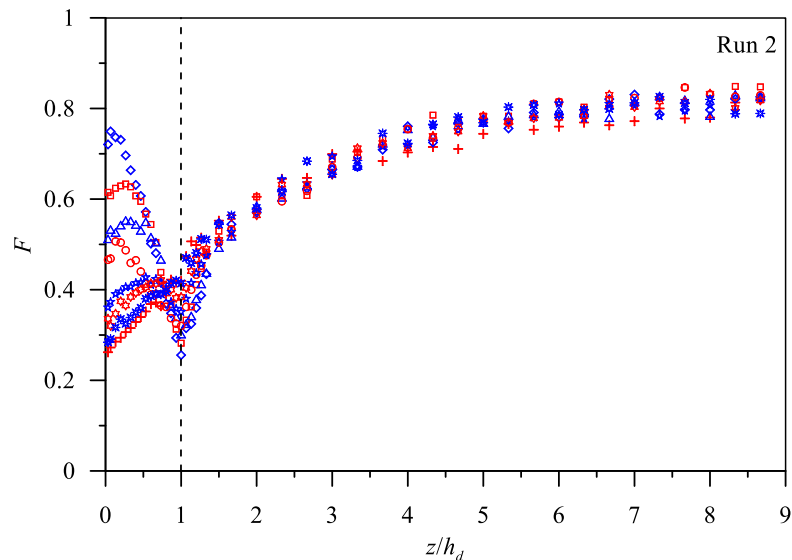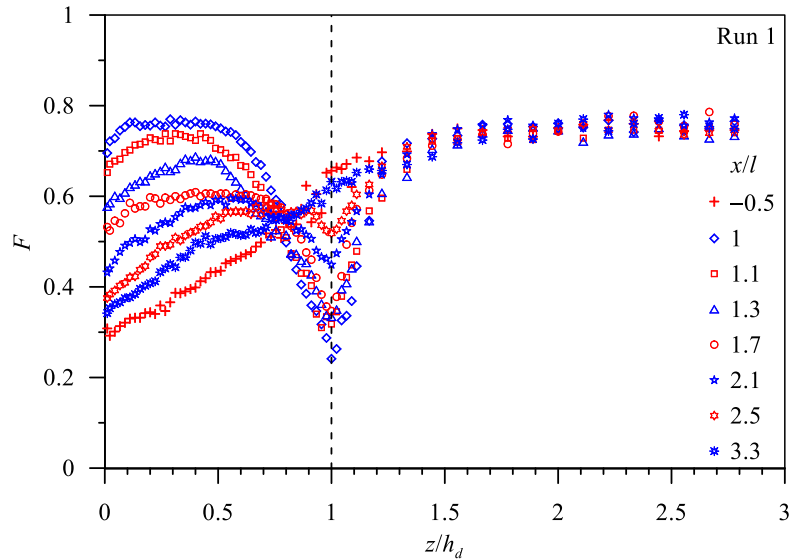
$$\mathbf{F} = 1 + 9I_2 + 27I_3$$
$$\mathbf{F} = 0: \text{two-component limit}$$
$$\mathbf{F} = 1: \text{3D isotropic state}$$

Fig. 16 Vertical profiles of anisotropy invariant function **F** at different streamwise distances for Runs 1 and 2

38

Upstream of the dune ($x/l = -0.5$), the data plots have a tendency to start with a two-dimensional isotropy from the near-bed flow and move monotonically toward a quasi-three-dimensional isotropy, as the vertical distance increases

Downstream of the dune, below the crest, the data plots in wall-wake flow have an affinity to a two-dimensional isotropy. Above the crest, as the vertical distance increases, the data plots sharply move toward a quasi-three-dimensional isotropy

The cusps formed by the anisotropy invariant function curves at the crest level in the wall-wake flow gradually disappear with an increase in downstream distance

Conclusions

The main findings are as follows:

The velocity in wall-wake flow downstream of an isolated dune suffers from a defect, where the Reynolds shear stress enhances owing to the fluid mixing

The wall-wake flow has a high-turbulence level with a peak at the dune crest. This level continues with the vertical distance until the effects of the dune vanish

The average traveling distance of turbulent eddies in wall-wake flow is greater than that in undisturbed upstream flow, while the length scales of turbulent eddies in the inertial subrange and dissipation range are smaller

In Reynolds stress anisotropy analysis, the AIMs illustrate a looping trend of data plots in wall-wake flow

Below the crest, the data plots show an affinity to a two-dimensional isotropy. It implies that an oblate spheroid axisymmetric turbulence is predominant with an axisymmetric contraction to increase with vertical distance up to the crest

Above the crest, the data plots show an affinity to a quasi-three-dimensional isotropy. It implies that an axisymmetric contraction to oblate spheroid reduces, as one goes toward the free surface

THANK YOU